ISSN (Print) 1226-1750
ISSN (Online) 2233-6656
Journal of Magnetics 18(2), 125-129 (2013) http://dx.doi.org/10.4283/JMAG.2013.18.2.125

Water-Cooled Direct Drive Permanent Magnet Motor Design in Consideration of its Efficiency and Structural Strength

Ji-Young Lee[1]*, Do-Kwan Hong[1], Byung-Chul Woo[1], Kyu-Seob Kim[2], and Jung-Pyo Hong[2]

[1]*Korea Electrotechnology Research Institute, Changwon 642-120, Korea*
[2]*Department of Automotive Engineering, Hanyang University, Seoul 133-791, Korea*

(Received 28 January 2013, Received in final form 3 May 2013, Accepted 8 May 2013)

This paper deals with a water-cooled direct drive permanent magnet (DD-PM) motor design for an injection-molding application. In order to meet the requirements for the target application and consider the practical problems of the manufacturing industry, the DD-PM motor is designed in consideration of efficiency and structural strength with many constraints. The performances of the designed motor are estimated not only by magnetic field analysis, but also by thermal and structural analysis. The design and analysis results are presented with experiment results.

Keywords : motor design, permanent magnet, structural strength, thermal analysis, water-cooling

1. Introduction

Permanent magnet (PM) synchronous motors having rare-earth magnets are widely used in many industrial applications due to their high torque density and high efficiency. Among various types of stator windings, a multi-pole fractional-slot concentrated-winding shows promise as a direct-drive motor [1-4]. In several rotor topologies, an interior PM (IPM) rotor structure has become popular as it can achieve higher torque density and efficiency. There is even an example where an IPM rotor [1] is being applied for injection-molding similarly to the application within this paper. However, an IPM rotor is mostly in a better position when used for traction application with a wide speed range. If the speed is low and the range is limited, the torque density and efficiency of surface PM (SPM) rotors are better than those of IPM rotors [4-6].

Therefore, this paper presents a design of a direct drive (DD) motor with an SPM rotor for injection molding application, with a speed rate of 250 rpm and output power of 55 kW. The machine is referred herein as a DD-PM motor. In order to meet the requirements of the target application and to consider the limited dimensions due to the practical problems associated with cost saving, the machine is designed in consideration of its efficiency and structural strength under many constraints. While the design process is presented, it focuses on an explanation of analysis and computation methods which are mainly required in each design stage.

©The Korean Magnetics Society. All rights reserved.
*Corresponding author: Tel: +82-55-280-1416
Fax: +82-55-280-1490, e-mail: jylee@keri.re.kr

2. Specifications and Design Process

2.1. Design Specifications and Conditions

The main design specifications for the target application are listed in Table 1, and the required torque during a typical operating cycle is as shown in Fig. 1. According to the required performances, the design aim is to maximize efficiency while maintaining the desired torque density. The presented dimensional constraints means that the stator core dimensions are fixed because of using the stator core which has already been fabricated for another application. The diameter of the stator core is relatively small, but it is used for costsaving when considering the manufacturer's practical problems.

2.2. Design Process

Electro-magnetic, thermal, and mechanical analyses are all required to complete this motor design. Electro-magnetic field analysis is necessary to meet motor performances such as torque and efficiency. Thermal analysis is needed due to the expectations of high current density, and mechanical analysis is required for the long expected

© 2013 Journal of Magnetics

Table 1. Design requirements and restrictions.

Items		Values	Units
Required Performances	Rated power	55	kW
	Rated torque	2100	Nm
	Max torque	2300	Nm
	Rated speed	250	rpm
	Torque ripple	< 5	%
	Efficiency at rated conditions	> 80	%
Dimensional constraints	Stator outer diameter	300	mm
	Rotor inner diameter	100	mm
	No. of stator slots	18	
	Air-gap length	1.0	mm
Material constraints	PM remanence at room temperature	1.3	T
	Type of lamination steel	35PN440	
	Coil fill-factor	< 40	%
	Cooling	Water cooling	
Limitations on power circuit	Input voltage	380	Vrms/line
	Output voltage	184	Vrms/ph
	Current limit	< 200	Arms

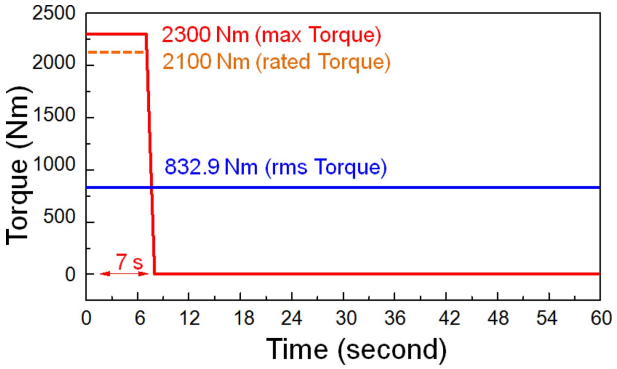

Fig. 1. (Color online) Required torque during a typical operating cycle.

stacking lengths under severe environments such as high temperature and torque.

Fig. 2 shows the flowchart for the design of the DD-PM motor. After confirming the design constraints and variables, parametric design is performed. For the one selected model, three consecutive analyses are performed: electro-magnetic, thermal and mechanical analysis. In the latter half of the design process, it must be verified whether the design results satisfy the restrictions through thermal and structural analysis. If the results are not satisfactory, the process returns back to the parametric design.

2.2.1. Classification of constraints and variables

Since the stator core is already fixed, the constraints and variables are classified as follows:

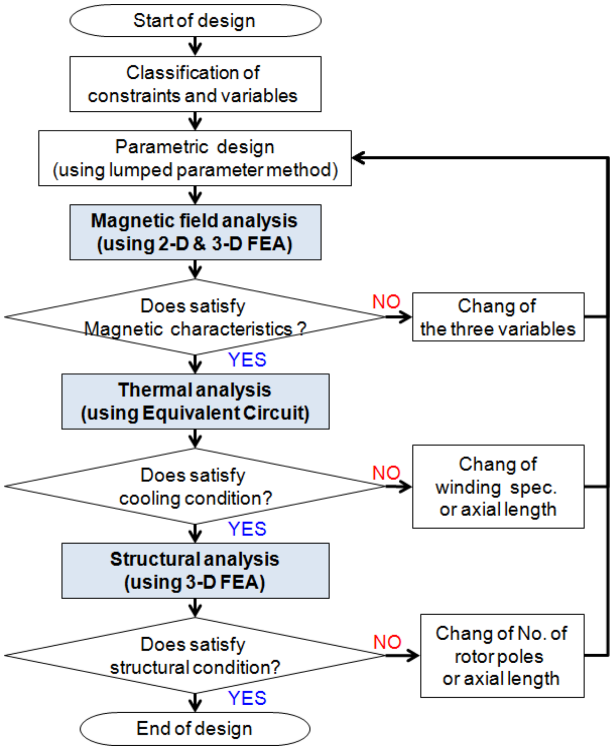

Fig. 2. (Color online) Flowchart of design process.

– Constraints: all stator dimensions except axial length, and materials as listed in Table 1.
– Design variables: number of rotor poles, winding specifications, and stack length.

During the design process, the number of rotor poles is investigated first because the pole-slot-combination is high-

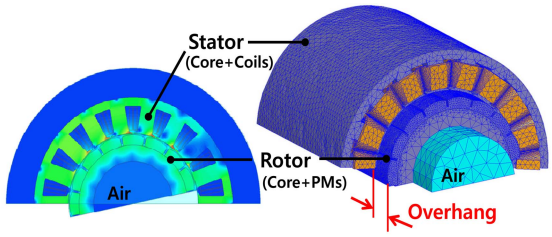

(a) flux density distribution in 2-D model (b) meshed 3-D model

Fig. 3. (Color online) 2-D and 3-D FEA models (16-pole 18-slot).

ly influential on motor performances [7]. Next, the winding specifications and stack lengths are selected in order to meet the design aim. The design variables are then decided through parametric design methods.

2.2.2. Parametric design and magnetic field analysis

The electro-magnetic parameters and performances, such as torque, induced voltage, inductance, etc., are computed by using three different methods: lumped parameter method, 2-dimensional (2-D), and 3-D finite element analysis (FEA) methods.

In the parametric design stage when dealing with several design variables, a lumped parameter method is used to narrow down the range of design variables. Thereafter, most of the magnetic field analysis is performed by voltage driven 2-D FEA, and the results are very reliable and sufficient in longitudinal flux machines with long axial-lamination cores. However, if the machine has an overhang with a different axial length between stator and rotor cores, the 3-D FEA method will be required.

Since the overhang is considered to improve torque density and efficiency, both 2-D and 3-D FEA methods are used in the design process, and each analysis model is shown in Fig. 3. The electro-magnetic parameters, such as torque, core and copper losses, and efficiency, are calculated from the results of magnetic field analysis, and thus, the main equations and related theories are arranged in [8].

2.2.3. Thermal analysis

In order to estimate the temperature of the DD-PM motor, a thermal equivalent circuit is used. The main equations and the related theories are presented in [9-11], and the thermal equivalent circuit network of the IPM motor in [11] was modified and used for this research. In thermal equivalent circuit network, the linear differential equation for the node can be derived as (1) [11].

$$C_i \frac{dT_i}{dt} = \frac{1}{R_{ji}}(T_j - T_i) + g_i \quad (1)$$

Table 2. Constants and coefficients for thermal analysis and structural analysis.

Material	Thermal conductivity (W/m·°C)	Young's Modulus (10^9 Pa)	Poisson's Ratio
Steel (35PN440)	50	195	0.25
Copper	380	110	0.34
Magnet	9	153	0.24
Epoxy resin	0.15	20.7	0.30
Aluminum	130	71.7	0.33
	Convection coefficient (W/m^2·°C)		
Housing outside	2124 (water cooling)		
Air-gap side	97 (air-cooling)		

where C_i is the ith node thermal capacitance, T_i is the ith node temperature, R_{ji} is thermal resistance between two adjacent nodes, and i, j and g_i is heat generation at node i. As compared with the thermal equivalent circuit network of the IPM motor, the three mainly modified lists are follows.

– Firstly, the thermal resistance of rotor part consists of rotor-I (rotor yoke) and magnet only. Since the DD-PM motor has a SPM rotor, the thermal resistances of flux barrier tip and rotor II (covers of PMs) are omitted.
– Secondly, radiation and forced convection by water-cooling are considered for housing surface with a water jacket. The water-cooling condition is computed for a coolant speed of 1 m/s in the axial direction. The constants and coefficients for thermal analysis are listed in Table 2.
– Thirdly, as in the thermal sources, only copper and core losses are considered whereas the application for low speeds, the eddy-current loss of PM is not considered.

As shown in Fig. 1, the graph for the required motor performance during a typical operating cycle for injection molding is pulse waveform. In the target application for this research, the short time duty is 7 seconds for a 1-minute cycle, and the maximum required torque is 2300 Nm. The virtual value (root-mean-square) of torque is calculated for the cycle, and then the corresponding current is computed. For the thermal analysis, the corresponding current is used for a calculation of copper losses.

2.2.4. Structural analysis

The equivalent stress is calculated in order to estimate the structural strength of the rotor. The von Mises stress is computed by FEA to determine mechanical equivalent stress. The main equations and the related theories are arranged in [8] and [12], and the constants for structural analysis are listed in Table 2 with the constants for thermal

Table 3. Winding factor, LCM, and analysis results according to number of pole (no. of slot = 18, torque = 2.2 knm).

No. of poles	Winding factor, kw	LCM	Analysis results		
			Cogging torque (Nm)	Torque ripple (%)	Efficiency (%)
14	0.902	126	7.68	0.62	75.7
16	**0.945**	**144**	**5.28**	**1.53**	**77.8**
20	0.945	180	5.12	1.89	77.8
22	0.902	198	4.18	2.00	75.7
24	0.866	72	38.06	5.67	74.6

analysis.

The following three cases are considered in order to check the mechanical stability of the rotor under severe environments:

– Case-1: rotating with a speed twice that of the rated speed
– Case-2: rotating with a rotor temperature of 100ºC
– Case-3: rotating with a torque level twice that of the rated torque with one end-frame fixed

3. Design and Analysis Results

3.1. Parametric design and magnetic field analysis results

Among the three design variables, the number of rotor poles was selected first. Table 3 shows the characteristics according to variations of the number of rotor poles in conditions with a torque of 2.2 kNm. Taking into consideration both torque ripple and efficiency, a 16-pole is selected as the best combination with the 18-slot in this table. The torque condition is satisfied here, but the efficiency does not meet the requirements.

The other design variables, winding specifications and stack length, are also being decided upon in order to improve efficiency. Fig. 4 shows efficiency variations according to stack lengths and numbers of coil turns, which are calculated with analysis results using the lumped parameter method. When the parallel circuit is one and the number of turns per coil is 10, efficiency is higher throughout the overall range.

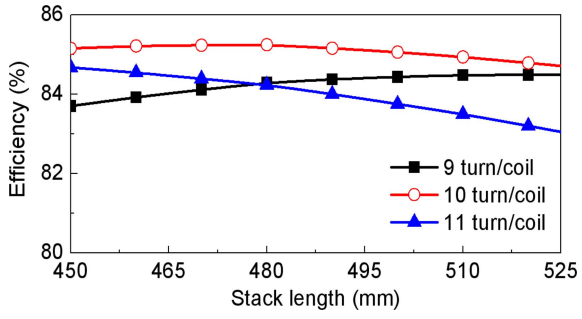

Fig. 4. (Color online) Efficiency according to stack length and number of coil turns variations, calculated by lumped parameter method.

Table 4. Design results and the performances.

Items			Values	Units
Design results	No. of rotor poles		16	
	No. of turns/phase		60	Turns
	Fill factor		39.8	%
	Current density		19.2	A/mm^2
	Phase resistance	Calculation	**0.12**	Ohm
		Measurement	**0.11**	
	Lamination-axial length	Stator	500	mm
		Rotor	540	mm
Performance (at 250 rpm)	Induced line -voltage const.	Calculation	**0.81**	V/rpm
		Measurement	**0.76**	
	Torque		2.31	kNm
	Output power		60.5	kW
	Copper loss		11.7	kW
	Core loss		0.2	kW
	Efficiency		83.6	%

The induced line voltage constant values are quite different between the calculation and measurement results. It is because of excessive parallel circuits in the fabricated motor. When the numbers of pole and slot are 16 and 18 respectively, the greatest common divisor is '2' and the possible parallel circuit is also the number '2'. It is possible that a winding tooth is made with several parallel connections of coils, but the parallel circuit of each phase should less than two. However, the fabricated machine has 6 parallel circuits per phase for easy winding, and the circulating currents in the parallel circuits make losses which decrease the induced voltage according to speed. In spite of the different parallel circuit, the resistance could be similar if the number of serial turn per phase and fill factors are the same between calculation and fabrication.

Based on a stack length of 480 mm, 2-D FEA is performed depending on stack length variations. Then, 3-D FEA is performed considering overhangs to improve efficiency. Finally, the results are obtained as shown in Table 4.

3.2. Thermal and structural analysis results

For the dimensions in Table 4, thermal analysis is performed with the sources of copper and core losses, and the results are shown in Fig. 5. The temperature in the end coil is steeply increased and saturated around 170 ºC. If H-grade, which has the maximum permissible temperature of 180 ºC, or the higher graded conductors are used,

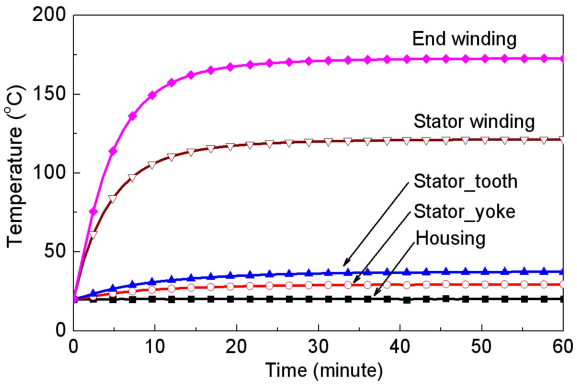

Fig. 5. (Color online) Thermal analysis results.

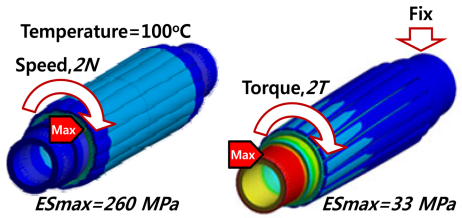

(a) Case-1 and Case-2 (b) Case-3

Fig. 6. (Color online) Equivalent stress analysis results (*2N*: two times of the rated speed, *2T*: two times of the rated torque, *ESmax*: max equivalent stress).

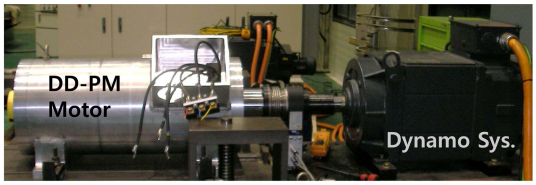

(a) DD-PM motor on dynamo system

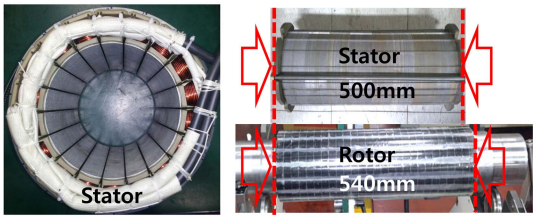

(b) front view of stator (c) side view of stator and rotor

Fig. 7. (Color online) Fabricated DD-PM motor.

the temperature of the end coil will not be considered. Except in the case of winding parts, the temperatures of other parts are saturated at around room temperature.

In the structural analysis, the previously mentioned three cases are investigated. Fig. 6 shows two results, where the left-side equivalent stress distribution is under conditions of both Case-1 and Case-2, and the other-side is about Case-3. Even the maximum stress is within the guaranteed value of the normal conditions between the PM and the rotor core. The yield point of the material 35PN440 is 324 MPa, whereas Fig. 6(a) shows that the maximum equivalent stress is 260 MPa on lamination steel.

4. Conclusions

As proposed in this design process, a DD-PM motor design was completed. The basic motor performances and its efficiency were verified by magnetic field analysis, and the structural strength was verified by thermal and structural analysis. Based on the design and analysis results, a DD-PM motor was fabricated as shown in Fig. 7, and the test results are being compared with calculated results in Table 4. Due to the excessive parallel circuit of windings, sufficient tests cannot be performed at the rated speed. However, the proposed design procedure could be a guidance for the PM motor design especially for water-cooled DD motor applications.

References

[1] Y. Kano and N. Matsui, IEEE Trans. Industry Appl. **44**, 543 (2008).
[2] R. Wrobel and P. H. Mellor, IEEE Trans. Energy Conver. **23**, 1 (2008).
[3] F. Magnussen and C. Sadarangani, IEMDC 2003, (2003) pp. 333-339.
[4] G. W. Cho, W. S. Jang, K. B. Jang, and G. T. Kim, J. Electrical Engineering & Technology **7**, 753 (2012).
[5] A. J. Rix and M. J. Kamper, IEEE Trans. Ind. Electron. **59**, 2475 (2012).
[6] A. Wang, Y. Jia, and W. L. Soong, IEEE Trans. Magn. **47**, 3606 (2011).
[7] J. Y. Lee, D. H. Koo, S. R. Moon, and C. K. Han, IEEE Trans. Magn. **48**, 2977 (2012).
[8] J. Y. Lee, D. K. Hong, B. C. Woo, D. H. Park, and B. U. Nam, IEEE Trans. Magn. **48**, 915 (2012).
[9] P. H. Mellor, D. Roberts, and D. R. Turner, IEE Proceedings-B **138**, 205 (1991).
[10] S. T. Lee, H. J. Kim, J. H. Cho, D. S. Joo, and D. K. Kim, J. Electrical Engineering & Technology **7**, 905 (2012).
[11] B. Lee, K. Kim, and J. Hong, IEEE Trans. Magn. **48**, 2949 (2012).
[12] D. K. Hong, B. C. Woo, and D. H. Koo, IEEE Trans. Magn. **45**, 2831 (2009).